NASA TECHNICAL MEMORANDUM

NASA TM X- 71473

NASA TM X- 71473

APPLICATION OF SLAR FOR MONITORING GREAT LAKES TOTAL ICE COVER

by R J. Jirberg, R. J. Schertler, R. T. Gedney, and H. Mark
Lewis Research Center
Cleveland, Ohio 44135

TECHNICAL PAPER proposed for presentation at Interdisciplinary Symposium on Advanced Concepts and Techniques in the Study of Snow and Ice Resources Monterey, California, December 2-6, 1973

APPLICATION OF SLAR FOR MONITORING GREAT LAKES TOTAL ICE COVER

R. J. Jirberg
R. J. Schertler
R. T. Gedney
H. Mark
Lewis Research Center, National Aeronautics and Space Administration, Cleveland, Ohio 44135

ABSTRACT

A series of X-band SLAR images is presented showing the development and disintegration of the entire ice cover on Lake Erie during the winter of 1972-1973. Simultaneous ground truth observations and ERTS-1 photography establish accurate correlations of radar responses with ice conditions. The all-weather, broad areal mapping capability of SLAR is seen to be the means for obtaining the repeated coverage needed for winter navigation on the Great Lakes.

INTRODUCTION

The success of current efforts to demonstrate the feasibility of extending the Great Lakes shipping season into the winter months hinges on a number of factors, not the least of which includes improvements in ice information techniques. To facilitate navigation by optimizing shipping routes through ice-bound waters, it is imperative that quick, accurate, and comprehensive appraisals of the ice cover be made available to shippers on a timely basis. In view of the tremendous areal extent of the ice cover and the need for repeated, in some cases daily, reconnaissance, it is clear that automated surveillance is the only viable approach. Among the various imaging devices under consideration for such an automated system, side-looking airborne radar (SLAR) offers two important advantages. One is the ability of the microwave radiation to penetrate all but the most severe weather, day or night. The other is its ability to map much broader swaths from aircraft altitudes than is possible with optical systems.

There have been a few investigations concerning the use of SLAR for ice monitoring beginning early in the 1960's mostly dealing with Arctic ice. From the onset it was apparent that the interpretation of the radar image in terms of the ice types and thickness would be the critical difficulty. Image analysis has been hampered both by a general lack of "ground truth" and by the absence of an accurate analytical model for the scattering of microwave radiation by the ice. Thus a continuing effort involving coordinated ground truth operations and SLAR overflights was launched to firmly establish the connection between the radar image and ice types. Through the cooperation of helicopter teams attached to the 9th District U.S. Coast Guard, it was possible in the first year of this effort to make some of the needed on-the-ice observations and thickness measurements in Lake Erie and in the Whitefish Bay area of Lake Superior. In the course of the study it became obvious that some of the previously held interpretations of radar imagery as to

ice type and thickness made without benefit of ground truth were inaccurate.

The SLAR used in this study was the Motorola AN/APS-94C system developed for the U.S. Army and flown aboard a Grumman Mohawk OV-1B. It operates in the X-band at 9.2 GHz on a real aperture principle with horizontal transmit and received polarization. Two previous SLAR studies of fresh-water ice have been reported, one by the U.S. Coast Guard (1972) using the Ku-band AN/DPD-2 system, and the other by Larroew et al. (1971) of Michigan's Willow Run Labs (now ERIM) using an X-band synthetic aperture system. The unique feature of the AN/APS-94C system among these and other present day SLAR systems is its extremely broad range of coverage--a capability that makes it feasible to repeatedly map areas as extensive as the Great Lakes.

LAKE ERIE TIME-LAPSE IMAGES

The broad mapping capability of the SLAR is illustrated in the series of images (Figures 2, 3, and 4) showing the entire ice cover on Lake Erie for the period from February 22 through March 5, 1973. This series of SLAR flights was preceded by a rare cloud-free look at the area by the ERTS-1 satellite as shown in Figure 1. Although four days had elapsed between the SLAR flight on the 22nd and the ERTS-1 pass, the correlation of features is striking. The influence of the winds is clearly evident. Note for example that northerly winds prior to the 18th had pushed the ice pack against the southern shore, carrying a relic pattern of the northern shoreline to near mid lake. Between the 18th and the 22nd, southwesterly winds then had carried the ice against the bottleneck at Long Point and into the eastern basin. In the process an extensive network of pressure ridges developed which are seen on the radar image as the dominant lacy pattern.

The flight of the 23rd was terminated midway down the lake, but is important in showing the development of large leads in the western basin due to the continued westerly winds. It also shows the fracturing of the new ice pinned against Pelee Point. A shift of the winds to the northeast during the 25th to the 27th is seen to have shoved the entire ice pack westward, shearing it off at Long Point and at Pelee Point. On the 28th, southerly winds developed shoving the ice pack northward, producing numerous leads as shown in the March 1 image. Also about this time, temperatures rose above freezing. Consequently by the 5th the disintegration of the ice cover had become well advanced.

To the image interpreter these repetitive views can reveal in a way not possible to aerial observers or from aerial photographs the intricate dynamics of the ice. The history is needed to infer thickness information because ground truth observations verified that tonal relations in the image do not directly convey thickness information as sometimes implied in the visible. This can be illustrated by comparing the differences in response to the visible and microwave radiation for the various ice types and thicknesses shown in the pair of images in Figure 5. The various regions of smooth unbroken ice, though varying in thickness from 31 to 41 cm., produce similar dark radar imagery, but in the visible are distinctly different. The radar image, however, is more clearly able to distinguish the rough pancake ice north of Pelee Island which had become layered to a depth of 115 cm. Other bright return areas in

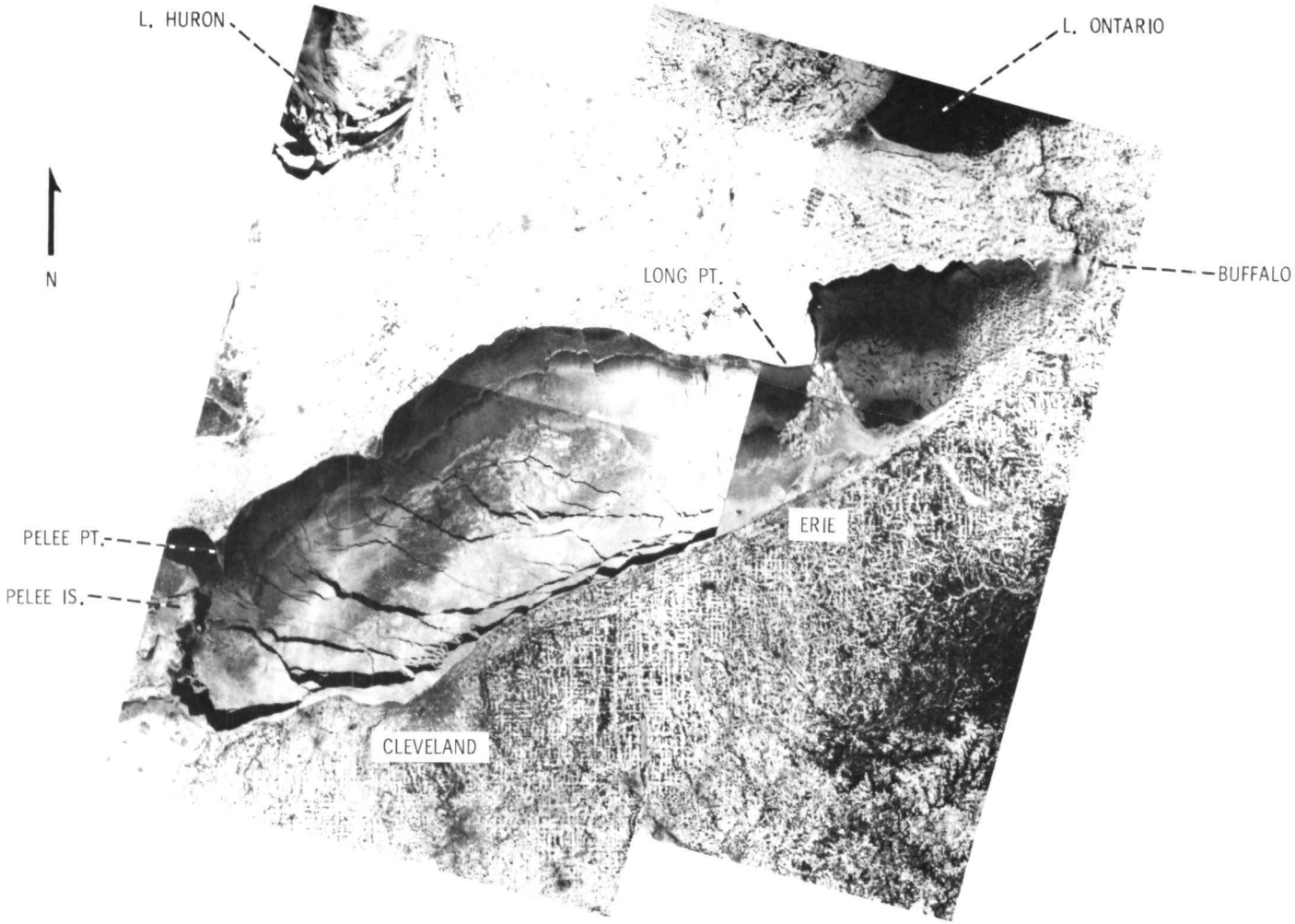

Figure 1. Photomosaic of ERTS-1 satellite imagery from band 4 showing Lake Erie ice cover on Feb. 17 (eastern basin) and Feb. 18, 1973 (central basin). Note the ice movement that occurred in one day along the southern shore.

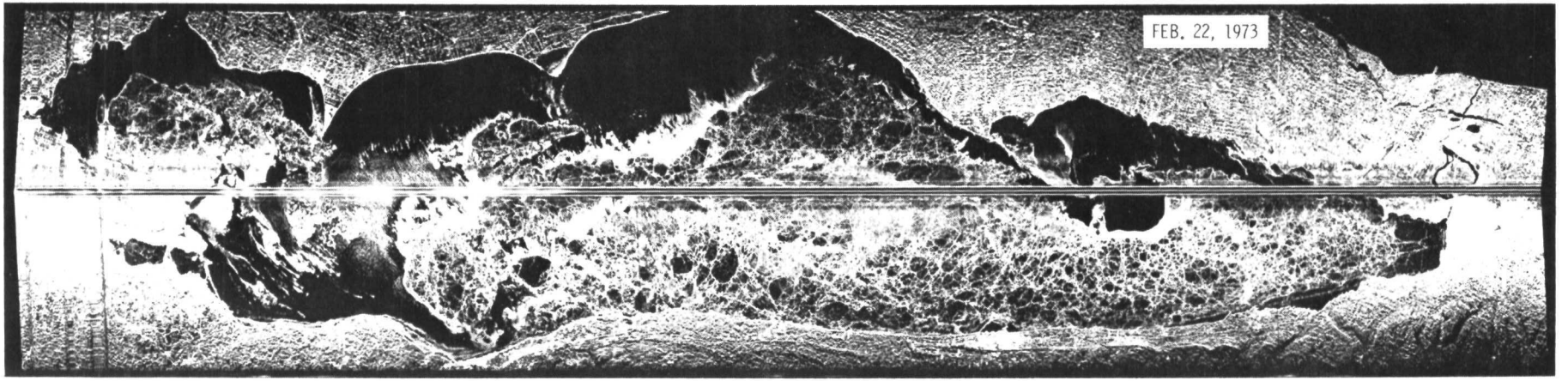

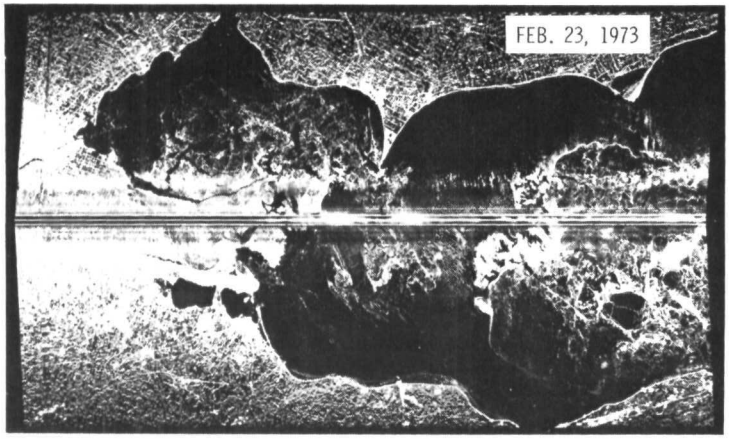

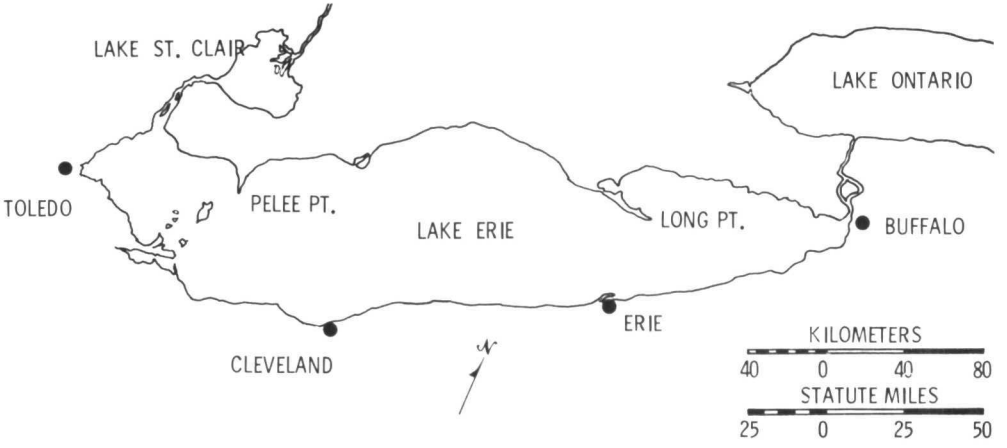

Figure 2. Radar images of Lake Erie ice cover on February 22 and 23, 1973. Time of flight over the lake was approximately 70 minutes. The center line of the image is the blind ground track of the aircraft.

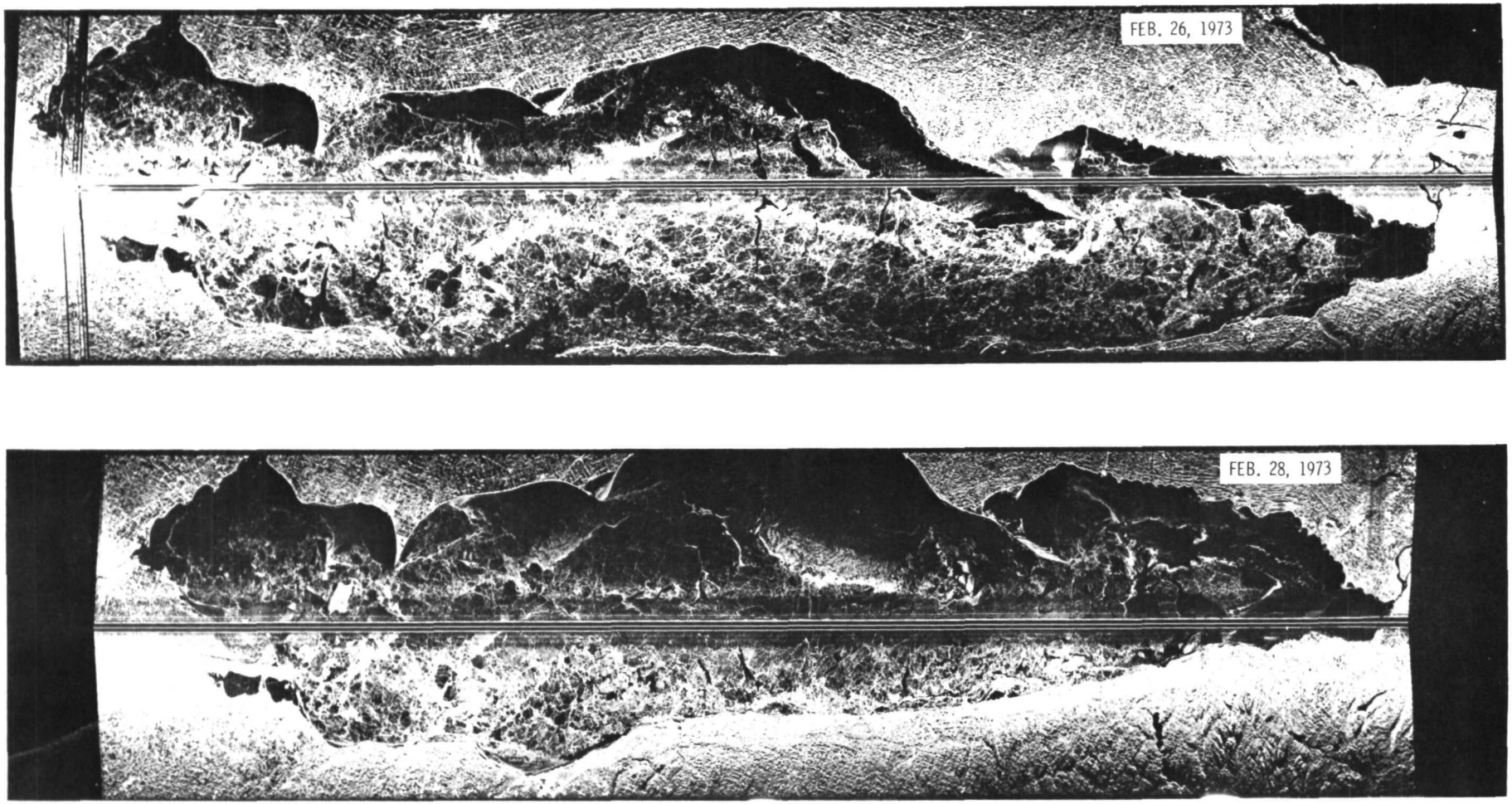

Figure 3. Radar images of Lake Erie ice cover on February 26 and 28, 1973. The compression of the image on the 28th resulted from an uncerfainty in ground speed. The distorted eastern end of the lake was due to a slight deviation in course.

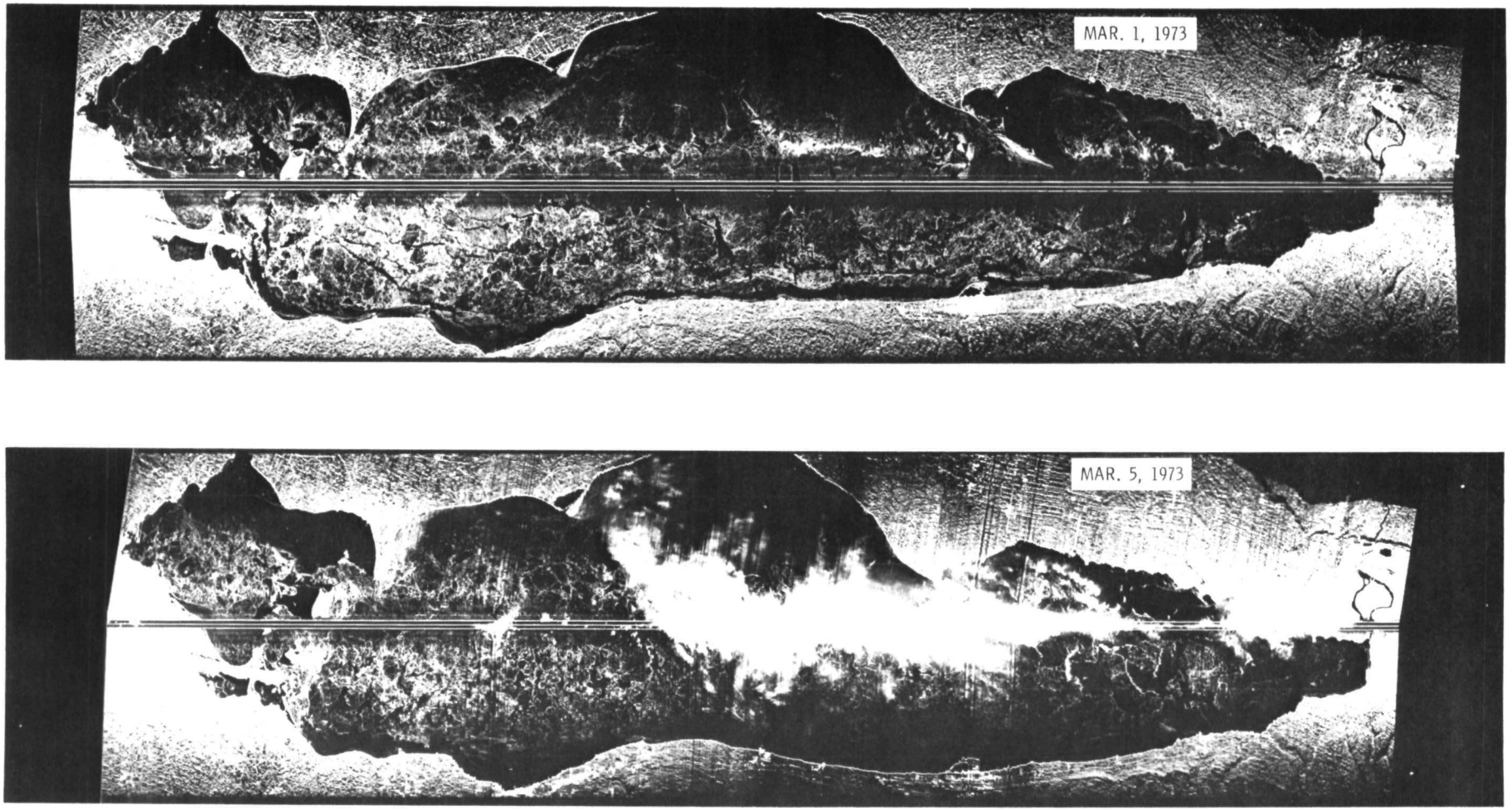

Figure 4. Radar images of Lake Erie ice cover on March 1 and 5, 1973. Rain and hail-filled clouds on the 5th which partially mask the ground were the only weather limitations encountered. Buffeting of the aircraft by strong gusty winds on the 5th produced some smearing of the image.

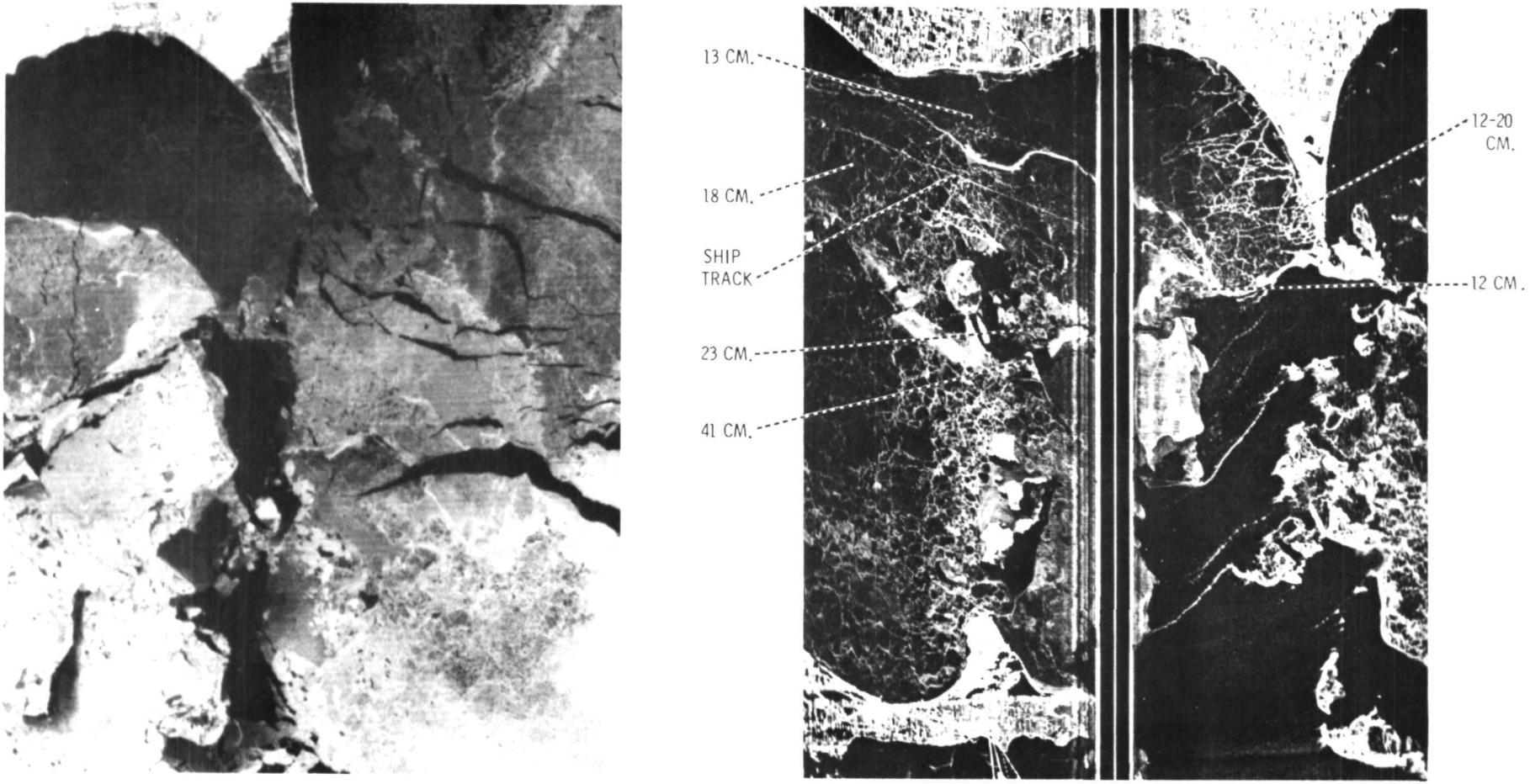

Figure 5. Western Lake Erie as seen from ERTS-1 in band 5 on Feb. 18, 1973 (left) and by SLAR (right) one day later. Pelee Island is prominent in the center with Pelee Point jutting down from the top.

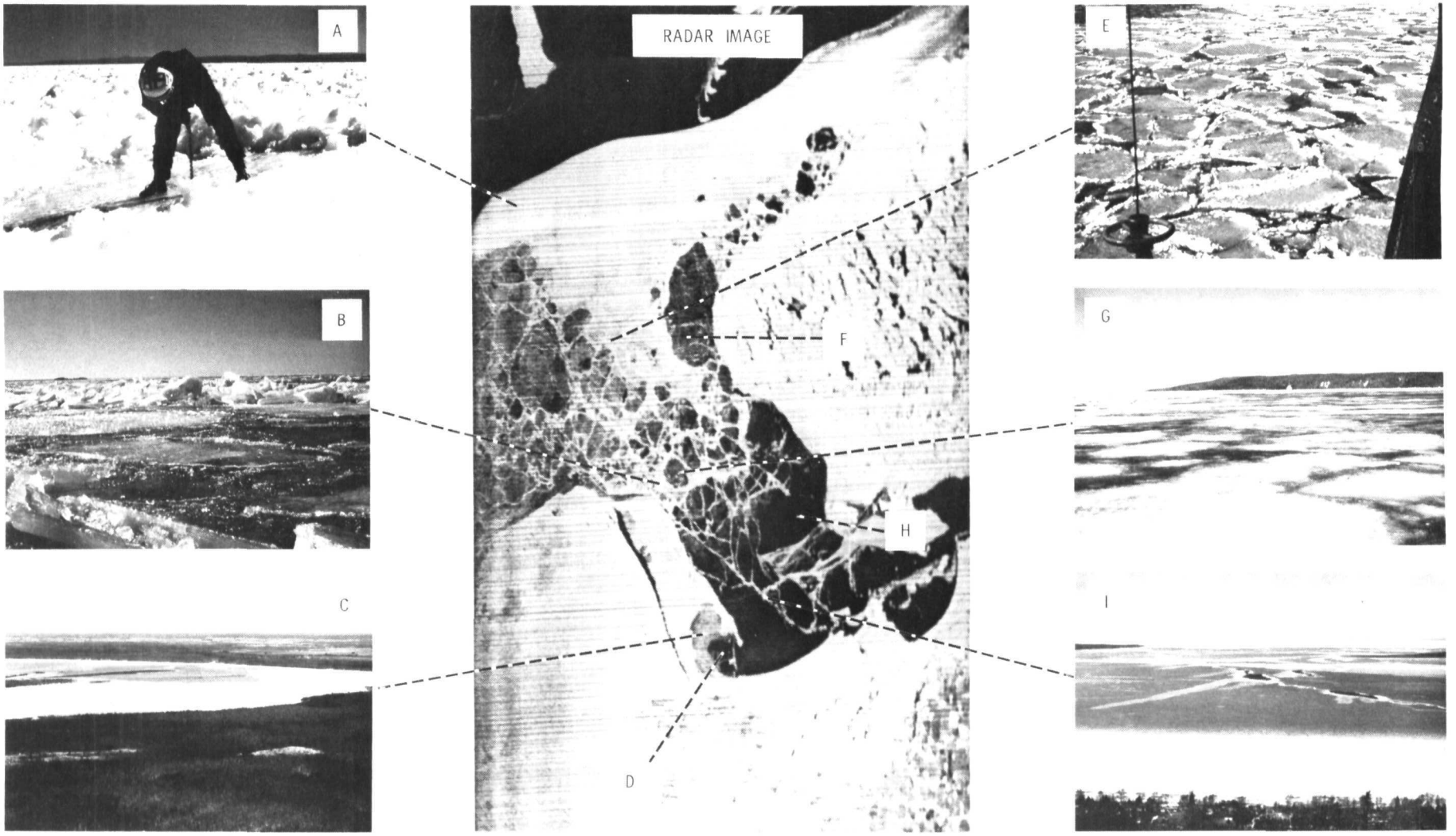

Figure 6. Whitefish Bay (L. Superior) ice cover on March 20, 1973 as mapped by SLAR and photographed at various ground truth test points.

E-7786

the SLAR image such as that off the tip of Pelee Point originate from regions of consolidated brash which, though deceptively smooth on the surface, had a stepped bottom profile which served as an effective radar reflector. This ice off Pelee Point was 15 cm. thick brash refrozen in a 10 cm. thick matrix.

WHITEFISH BAY GROUND TRUTH

Further indications of the nature of the microwave scattering by the ice were obtained in Whitefish Bay. In Figure 6, the medium-gray area at point C was found to be fast ice, 41 cm. thick, with a 1 or 2 cm. surface ripple. To the eye this area was milky white. The difference in returns between this ice and the adjacent ice at D is believed to be associated with the inclusions present in the fast ice that gave it its milky appearance rather than with the surface ripple. Unfortunately no detailed examination of this milky ice was made, but one possibility is that tiny voids (bubbles) are responsible for its appearance. The ice at D was similarly rippled, but being newer (10 cm. thick), was dark blue in color and unbroken except for fine hairlike cracks. Since this newer ice contained no appreciable scattering sites, it appears no different from the large open water area at H.

The long linear feature at I was a major pressure ridge. Although not an especially striking feature among the surrounding surface clutter when viewed at higher altitudes, its rafted edges make it a good radar target. The thickness of the surrounding ice sheet varied between 35 and 55 cm.

The high return area in and around point B was an area that had undergone considerable crushing, forming a ridged ice zone. The large cellular areas such as F and G were brash ice 44 to 50 cm. thick smoothly refrozen in a 28 cm. thick darker ice matrix. Here again, these cells were difficult to locate among the surface detail from altitude, but because of the microwave scattering off the stepped bottom profile, they clearly stand out in the radar image.

The area that includes point E was found to be composed of rafted angular plates of 32 cm. thick white ice, each on the order of 1 to 5 meters across, refrozen in 24 cm. thick dark ice. Ice build up on the edges of the plates gave the area a high degree of vertical roughness. The roughest ice was found at the edge of the ice pack at point A. Here, due to the constant lapping of the waves and the wind-driven spray, the surface had accumulated a globular foam-like coating of ice 40 to 60 cm. thick. Beneath was a layered accumulation of brash ice extending to depths in excess of 1 meter.

CONCLUDING REMARKS

Except for the case of fast ice (shore ice), it has become apparent that the radar "sees" a world of edges rather than one of bulk forms as we are used to in the visible. In the radar image, ice types such as brash, pancake, and related forms are often the brightest simply due to the large vertical cross section presented by their edges. Strong returns are also produced by ice types with a surface roughness of 10 cm. or more such as occur when edges are built up by wave and spray action, or as occur when ice debris is accumulated along pressure ridges. Similarly, ice types with a comparably rough bottom profile such as consolidated brash produce

strong returns due to penetration of the ice by the microwave radiation and its subsequent backscatter off ice-water corner interfaces. Only in the case of fast ice have we seen any indication of volume scattering such as gives us our visual impressions.

Further work is warranted to determine the microwave scattering cross sections for the various ice types and thus allow a better fix on the dynamic range of signals bearing useful information. With the sensitivity and video gain characteristics as designed into the AN/APS-94C system, it was not possible to discriminate unfractured ice from open water directly simply because smooth clear ice lacks sufficient defects to backscatter enough radiation to be detected. Also since clear ice is so transparent at X-band, the dominant sources of backscatter are the edges and ice-water corners rather than volume scatterers. This together with the fact that the density of scatterers can vary widely from one ice type to another, and may not always be correlated to ice thickness, hinders the discrimination of varied ice thicknesses. It remains to be determined to what extent a radar system calibrated in terms of the ratio of backscattered to incident radiation can resolve differences in returns from the various ice types and thicknesses. An additional source for thickness information may be in the degree of depolarization of the radiation with thickness of the ice as noted by Bryan and Larson (1973). Other clues as to ice thickness may be found in the way in which the ice yields to wind stress and in the way ice types develop with time.

Further effort is also warranted to correlate the impeding forces and other difficulties actually encountered by vessels transiting the ice to the information available in the radar image. It is significant that the rougher ice and especially brash ice which is among the most difficult to transit is also that which gives the strongest returns in the radar image. Feedback from shippers in this regard will be valuable.

REFERENCES

Bryan, M. L., and R. W. Larson, 1973. Application of dielectric constant measurements to radar imagery interpretation, Presented at the Second Annual Remote Sensing of Earth Resources Conference, University of Tennessee Space Institute, March 26-28, 1973.

Larrowe, B. T. et al., 1971. Fine-resolution radar investigation of great lakes ice cover. Final Report, Willow Run Laboratories, University of Michigan, January 1971.

U.S. Coast Guard, 1972. Analysis of SLAR imagery of Arctic and lake ice. Final Report, DOT-CG-14486-A, April 1972. Interpretation of winter ice conditions from SLAR imagery. Final Report, DOT-CG-14486-1A, February 1972.